Determination of band alignment of pulsed-laser-deposited perovskite titanate/III-V semiconductor heterostructure using X-ray and ultraviolet photoelectron spectroscopy

Zhibin Yang, Wen Huang, and Jianhua Hao

View Online   Export Citation   CrossMark

ARTICLES YOU MAY BE INTERESTED IN

In-plane dielectric properties of epitaxial $Ba_{0.7}Sr_{0.3}TiO_3$ thin films grown on GaAs for tunable device application
Journal of Applied Physics **112**, 054110 (2012); https://doi.org/10.1063/1.4749270

Electrical properties of ferroelectric $BaTiO_3$ thin film on $SrTiO_3$ buffered GaAs by laser molecular beam epitaxy
Applied Physics Letters **94**, 032905 (2009); https://doi.org/10.1063/1.3075955

Structural and resistance switching properties of $ZnO/SrTiO_3/GaAs$ heterostructure grown by laser molecular beam epitaxy
Applied Physics Letters **97**, 162905 (2010); https://doi.org/10.1063/1.3505136

Determination of band alignment of pulsed-laser-deposited perovskite titanate/III-V semiconductor heterostructure using X-ray and ultraviolet photoelectron spectroscopy

Zhibin Yang, Wen Huang, and Jianhua Hao[a)]

*Department of Applied Physics, The Hong Kong Polytechnic University, Hung Hom, Hong Kong,
People's Republic of China*

Techniques of X-ray and ultraviolet photoelectron spectroscopy are performed to investigate the energy band discontinuity of pulsed-laser-deposited $SrTiO_3$ (STO)/GaAs heterostructure. The valence band offset is determined to be 2.6 eV, while the conduction band offset is deduced to be 0.7 eV. As a consequence, an energy band diagram of STO/GaAs with a type II band alignment forming at the interface is precisely constructed. The chemical states across the STO/GaAs interface are investigated by sputter-depth profile, and there are no detectable interfacial reaction and intermediate layer occurring between the epitaxial STO film and GaAs substrate. © 2013 AIP Publishing LLC. [http://dx.doi.org/10.1063/1.4816356]

GaAs metal-oxide-semiconductor field-effect transistors (MOSFETs) with high-mobility have shown promising performance compared to Si-based devices. Much research has been focused on the electrical properties of GaAs-MOSFET with amorphous and polycrystalline dielectric oxide, including HfO_2, Ga_2O_3, Gd_2O_3, and so on.[1–3] Unfortunately, high density of dangling bonds are usually found at the oxide/GaAs interface.[4] GaAs MOS devices with epitaxial dielectric layers should have a low interface trap density of states, since a perfect epitaxial interface has stable interfacial chemical bonds.[5] Also, contrary to polycrystalline oxides, a perfect epitaxial oxide contains no grain boundaries, which preserves the desired features of the low leakage current and uniformity.[6]

Among several types of gate oxides, perovskite-type oxides, such as $SrTiO_3$ (STO), and $BaTiO_3$ (BTO) exhibiting both high-k and ferroelectric properties are one of promising dielectric oxides for high-performance GaAs-MOSFET.[7,8] However, epitaxial growth of these perovskite titanates directly on GaAs is rather challenging, since GaAs is neither chemically stable nor thermally stable at high temperature needed for the epitaxial growth of perovskite titanates.[9] In order to obtain epitaxial perovskite titanates, a single and/or multi-buffer layer is usually needed.[10–12] Ferroelectric properties in epitaxially grown BTO on GaAs via MgO buffer by molecular beam epitaxy (MBE) are reported to be greatly sensitive to the interface structure.[10] In BTO/MgO/Al_xO_y/GaAs heterostructure, primary optical confinement in the BTO thin film was also shown due to the interface chemical state of the heterostructure.[11] However, earlier study shows that the very thin MgO on GaAs may suffer from the high charge injection due to the trapped charge at interface.[12] In these epitaxial heterostructures, band alignment is a central issue for the understanding of perovskite oxide/GaAs interface, because it dictates many behaviors taking place in a device made up of these heterojunctions. Fermi level at the

interface of MBE grown STO/GaAs was found to be unpinned at the interface.[13] Very recently, the properties of MBE grown BTO/GaAs have been reported, in which the Ba and Ti atoms were fully oxidized in the films and the interface showed an evidence of unexpected Ga-O chemical bonding.[14] Compared to the MBE deposition, pulsed laser deposition (PLD) including laser MBE is much more commonly used, particularly suitable for the perovskite oxide deposition. Obviously, different growth mechanism and thin-film deposition conditions (temperature, growth rate, atmosphere, etc.) may vary chemical bonding and band alignment at the interface.[15] Therefore, it is interesting to investigate interfacial phase and understand the exact band alignment of the PLD grown perovskite titanate/GaAs. Unfortunately, there is a lack of such data available on the PLD grown heterostructure. In this letter, we report X-ray and ultraviolet photoelectron spectroscopy (XPS and UPS) studies on the interfacial structure characteristics of PLD grown STO/GaAs heterostructure, and subsequently the energy band diagram with band alignment is precisely constructed. Similar to the approach used for our earlier study on STO/Si,[16] the interfacial phase of the STO/GaAs heterostructure is also investigated.

p-GaAs (001) wafers with size of $10 \times 10 \times 0.5$ mm^3 were used as substrates. The STO films were prepared by using laser MBE. The optimum conditions for epitaxial STO thin film grown on GaAs substrates have been obtained in our previous report.[17,18] Briefly, the GaAs substrate was first *in situ* heated up to 620 °C in vacuum for 2 min to remove the native oxide layer. A single-crystal STO target was ablated using a KrF excimer laser. To prevent the GaAs substrate from oxidizing, the chamber was evacuated to a base pressure of 1×10^{-5} Pa during thin film deposition. The deposition temperature was set around 600 °C for STO thin-film deposition. The crystallographic characterization was performed by high-resolution X-ray diffractometer (HRXRD). The interfacial microstructures were studied using high-resolution transmission electron microscopy (HRTEM). The photoemission measurements of the valence band discontinuity of the

[a)]Author to whom correspondence should be addressed. Electronic mail: jh.hao@polyu.edu.hk

heterostructures were performed on the XPS and UPS systems with hemispherical electron energy analyzer, monochromatic Al Kα X-ray source and a He ultraviolet lamp. The depth profile of STO/GaAs heterostructure was obtained from XPS spectra as a function of sputtering time.

Figure 1(a) shows a typical θ-2θ XRD pattern from a 150 nm thick STO film epitaxial grown on GaAs (001) measured at room temperature. It indicates that the STO thin films have a cubic perovskite structure and are highly oriented along c-axis. Patterns shown in Figure 1(b) are the off-axis Φ scans of the STO film and GaAs substrates. The measured results suggest that the STO unit is epitaxially grown on GaAs with a 45° in-plane rotation to get a comfortable lattice match due to a large mismatch between STO(a = 3.905 Å) and GaAs(a = 5.65 Å), as shown in the schematic diagram (Fig. 1(c)), and thus the lattice mismatch after the rotation would be calculated to be ($|\sqrt{2}\alpha_{STO} - \alpha_{GaAs}|/\alpha_{GaAs}$) × 100% = 2.2%. Additionally, Figure 1(d) presents a cross-sectional HRTEM image of the epitaxial STO thin film on GaAs. The sharp interface transition is indicative of no obvious inter-diffusion and reaction between the STO film and the semiconductor GaAs substrate. The corresponding selected area electron diffraction (SAED) pattern shown in Figure 1(d) suggests the small lattice mismatch after a 45° in-plane rotation between STO and GaAs, which is consistent with the previous report.[17,18] The result confirms a highly epitaxial STO film grown directly on the GaAs substrate. However, periodic array of misfit dislocations can be observed in the interface area as marked with arrow heads in the TEM image, revealing that there is still lattice strain remained at the interface due to the lattice mismatch between STO film and GaAs substrate. In principle, the misfit location depends on the deposited film thickness. Prior to the complete relaxation of strain, it is believed that more dislocations could be generated to relieve the misfit strain when the film becomes thick.[19] The dislocation is not induced by self-energy but by reduction of the strain energy at the interface.[20] On the other hand, interfacial phase and chemical state between STO and GaAs could not be verified from the TEM analysis. Hence, XPS depth profiling will be carried out in later section to determine whether any interfacial compound is formed or not at the interface of STO/GaAs.

Figure 2 shows the core level (CL) spectra including Ti $2p_{3/2}$ and As $2p_{3/2}$ recorded on STO/GaAs samples with two different thickness (2 and 150 nm), as well as valence band (VB) spectra recorded on STO and GaAs. The CL spectra were fitted to Voigt (mixed Lorentzian-Gaussian) line shape by employing a Shirley background. As seen in Figure 2(a), the Ti atoms have been fully oxidized in the 4^+ oxidation state, and there is no peak at higher energy observed in earlier report.[13] A classic method was introduced to determine the band offsets of the STO/GaAs heterostructure.[21] The valance bands and CL of the clean GaAs surface and the STO/GaAs (001) are measured in the successive photoemission measurements. The valence band offset (VBO) **ΔE_v** can be calculated from the formula,

$$\Delta E_v = (E_{cl}^{GaAs} - E_v^{GaAs})^s - (E_{cl}^{STO} - E_v^{STO})^f + (E_{cl}^{STO} - E_{cl}^{GaAs})^{int},$$

(1)
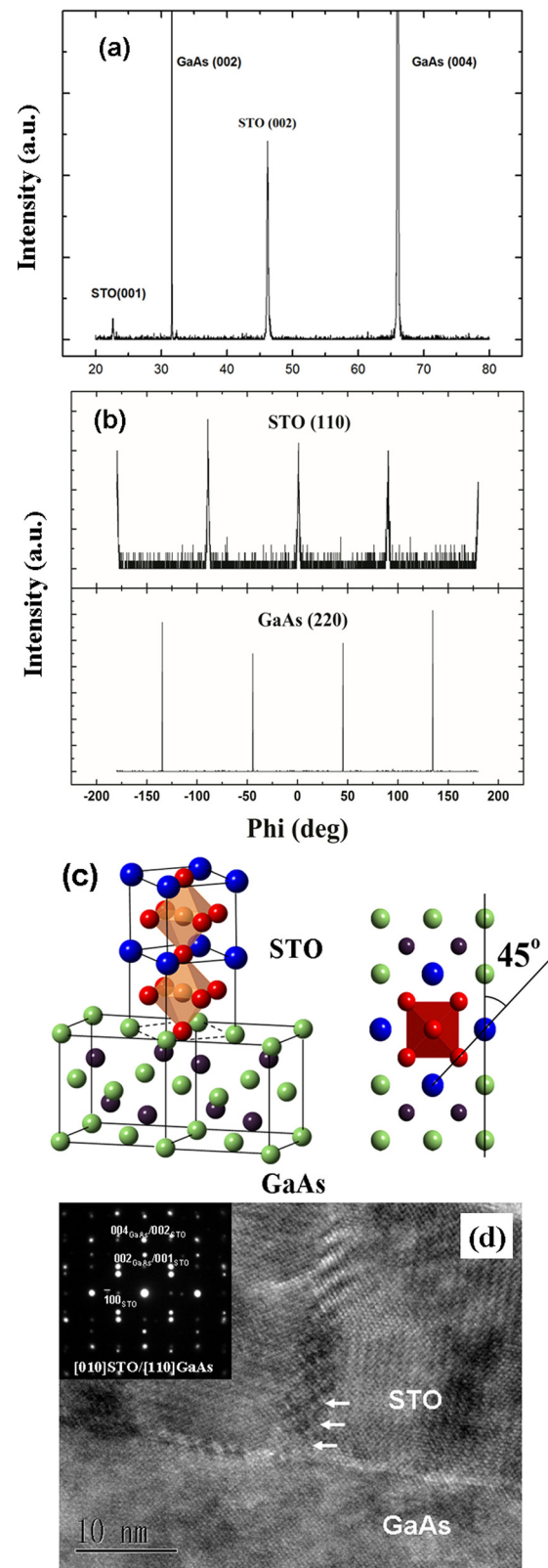
FIG. 1. (a) XRD pattern of θ-2θ scan of STO/GaAs (001) heterostructure measured at room temperature. (b) Phi scan of (110) reflections of the STO thin film and GaAs (220) substrate. (c) Schematic diagram of the STO/GaAs atomic interface structure. (d) Cross-sectional HRTEM image of STO/GaAs. The inset figure is the SAED pattern at the interface.

where $(E_{cl}^{GaAs} - E_v^{GaAs})^s$ and $(E_{cl}^{STO} - E_v^{STO})^f$ are the difference of the CLs and the valence band maximums (VBMs) of clean high-resistivity GaAs substrate and 150 nm thick STO film, and $(E_{cl}^{STO} - E_{cl}^{GaAs})^{int}$ is the difference of CLs between
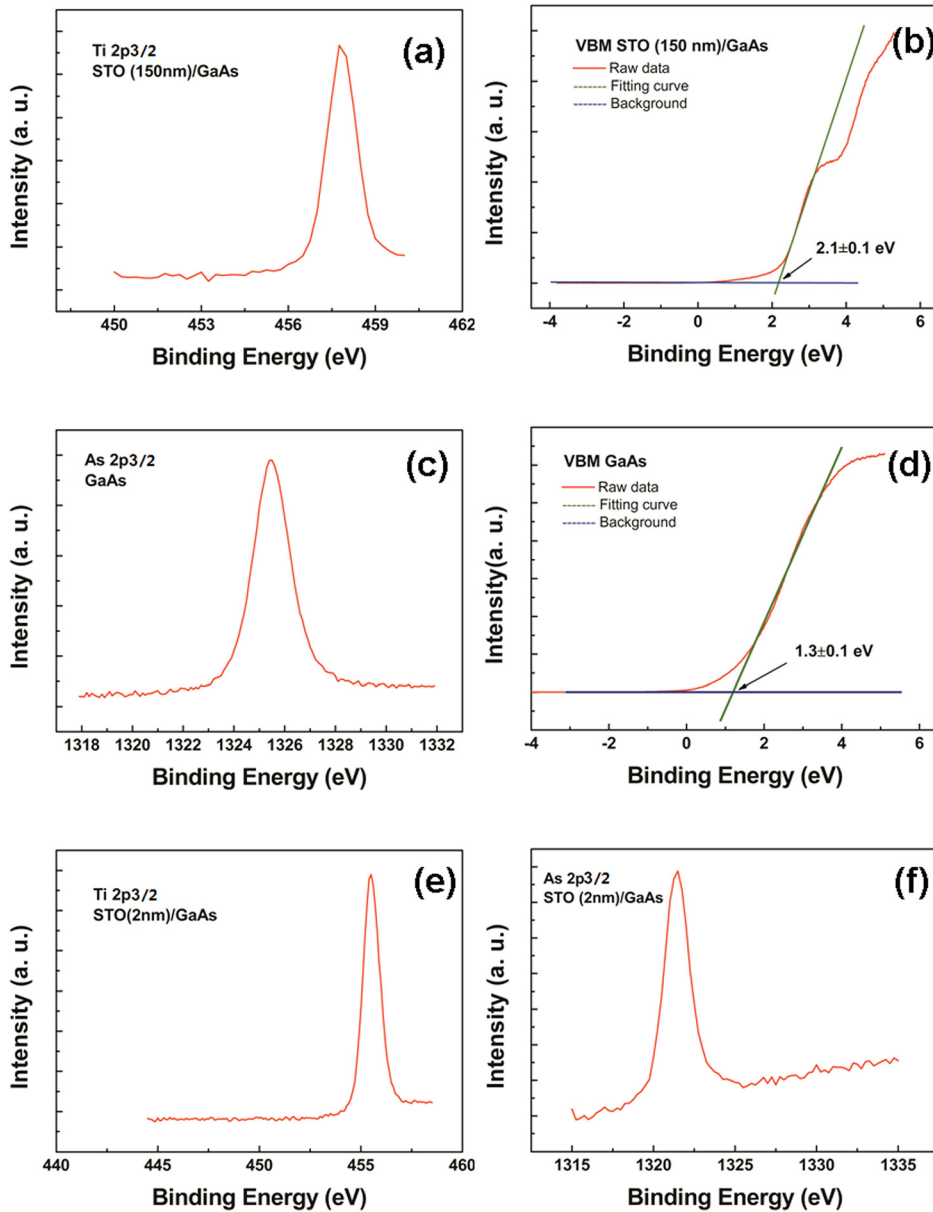
FIG. 2. XPS and UPS spectra of STO on GaAs. Core level Ti $2p_{3/2}$ spectra recorded on STO (150 nm) (a) and STO (2 nm)/GaAs (e), As $2p_{3/2}$ spectra on GaAs (c) and STO (2 nm)/GaAs (f), VB spectra for STO (b) and GaAs (d). All VBM values are determined by linear extrapolation of the leading edge to the base line.

the 2 nm thick STO thin film and GaAs substrate, respectively. In general, two steps were used to determine the VBO of the heterostructure in our study. First, the energy difference between the VBMs and CLs for both GaAs substrate and thick STO film was evaluated. VBMs and CLs were measured by UPS and XPS techniques, respectively. Second, the energy difference of CLs between STO film and GaAs substrate of STO/GaAs heterostructure was determined. Linear extrapolation of the XPS valence band edge was performed to calculate the VBM. As shown in Fig. 2, the CL position and VBM for the 150 nm thick STO film grown on GaAs are 457.7 ± 0.03 eV (Ti $2p_{3/2}$) (Fig. 2(a)) and 2.1 ± 0.1 eV (Fig. 2(b)), respectively. Furthermore, the CL position and VBM for the clean high resistivity GaAs substrate are 1325.5 ± 0.03 eV (As $2p_{3/2}$) (Fig. 2(c)) and 1.3 ± 0.1 eV (Fig. 2(d)), respectively. For the 2 nm thick STO film grown on GaAs substrate, the CL positions are 455.5 ± 0.03 eV for STO (Ti $2p_{3/2}$) (Fig. 2(e)) and 1321.5 ± 0.03 eV for GaAs (As $2p_{3/2}$) (Fig. 2(f)). The measured and fitting results are summarized as shown in Table I.

Hence, the separation between As $2p_{3/2}$ and Ti $2p_{3/2}$ for the STO (2 nm)/GaAs is about 866.0 eV. From the above values, the VBO of STO/GaAs can be calculated to be 2.6 eV, Moreover, the conduction band offset (CBO) can be obtained by using the formula,

$$\Delta E_c = (E_g^{GaAs} - E_g^{STO}) + \Delta E_v, \qquad (2)$$

TABLE I. XPS CL spectra fitting results and VBM positions obtained by linear extrapolation of the leading edge to extended base line of the VB spectra.

Sample	State	Binding energy (eV)
STO	Ti $2p_{3/2}$	457.7 ± 0.03 (Ti-O)
	VBM	2.1 ± 0.1
GaAs	As $2p_{3/2}$	1325.5 ± 0.03 (Ga-As)
	VBM	1.3 ± 0.1
STO/GaAs	Ti $2p_{3/2}$	455.5 ± 0.03 (Ti-O)
	As $2p_{3/2}$	1321.5 ± 0.03 (Ga-As)
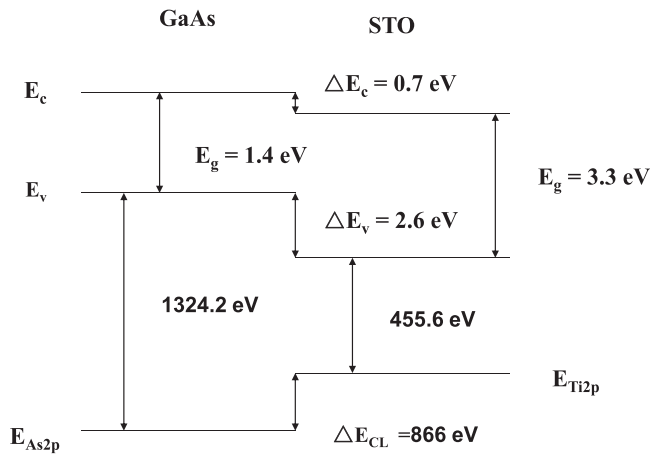
FIG. 3. Band alignment diagram of STO/GaAs heterojunction based on the XPS experimental and fitting results.

where ΔE_c represents CBO, E_g^{GaAs} represents the band gap of GaAs, and E_g^{STO} represents the band gap of STO. By considering the values of band gap for STO and GaAs are 3.3 and 1.4 eV, respectively, we can find the CBO of the heterostructure to be 0.7 eV. Our result is consistent with the VBO and CBO values measured from STO/GaAs heterojunction fabricated by MBE technique.[15] Our samples were fabricated by using laser deposition, in which a relatively higher growth temperature is used compared to MBE. It suggests that the band discontinuities are not greatly influenced by the growth method and deposition conditions, such as substrate temperature.

As the above values of both VBO and CBO in STO/GaAs are positive, the valence band and conduction band of the STO film are lower than those of the GaAs substrate. It suggests that STO/GaAs fabricated by laser MBE forms a type II heterostructure. According to the band alignment

from Fig. 2, the energy band diagram of the STO/GaAs can be constructed as shown in Figure 3. Such a type of band alignment across the interface is generally thought to be suitable for various applications in optoelectronic and high-power devices, which could enable electrons confined in the STO and holes in the GaAs transport across the interface efficiently by selecting proper metals as electrodes. However, according to the previous report,[13] initial Ti prelayer could react primarily with the surface As during film growth by MBE. The Ti-As intermediate compound could also be formed at the interface in BTO/GaAs heterostructure.[14] These interfacial bonding states induced by intermediate compound could be acted as the origin of the Fermi level pinning center at the interface in these covalently bonded semiconductors,[22] which may cause unexpected barrier heights to hinder the charge transport.

In order to clarify the interfacial chemical state of the STO/GaAs heterostructure prepared by laser deposition, the XPS depth profile of the interface was investigated. Figure 4 shows the core level spectra of our STO/GaAs sample. As shown in Fig. 4(a), the binding energies of Sr $3d_{5/2}$ and Sr $3d_{3/2}$ lines corresponding to Sr^{2+} are found to be 132.4 and 135.2 eV, respectively. The line profile remains almost unchanged except that the linewidth becomes larger. Particularly, no obvious line shift is observed when the probing depth crosses the STO/GaAs interface. The clear As $3p_{3/2}$ line is seen with the disappearance of the Sr $3d$ lines when the probing depth has crossed the interface and arrived in the GaAs wafer (Fig. 4(d)). It indicates that there is little change with the chemical state of Sr^{2+} throughout the STO/GaAs system. This finding excludes the possibility of the existence of a Sr metallic compound which would cause the Sr line shift ~2 eV in some systems, such as our previously studied STO/Si.[16,23] Moreover, the chemical state of Ti was characterized.
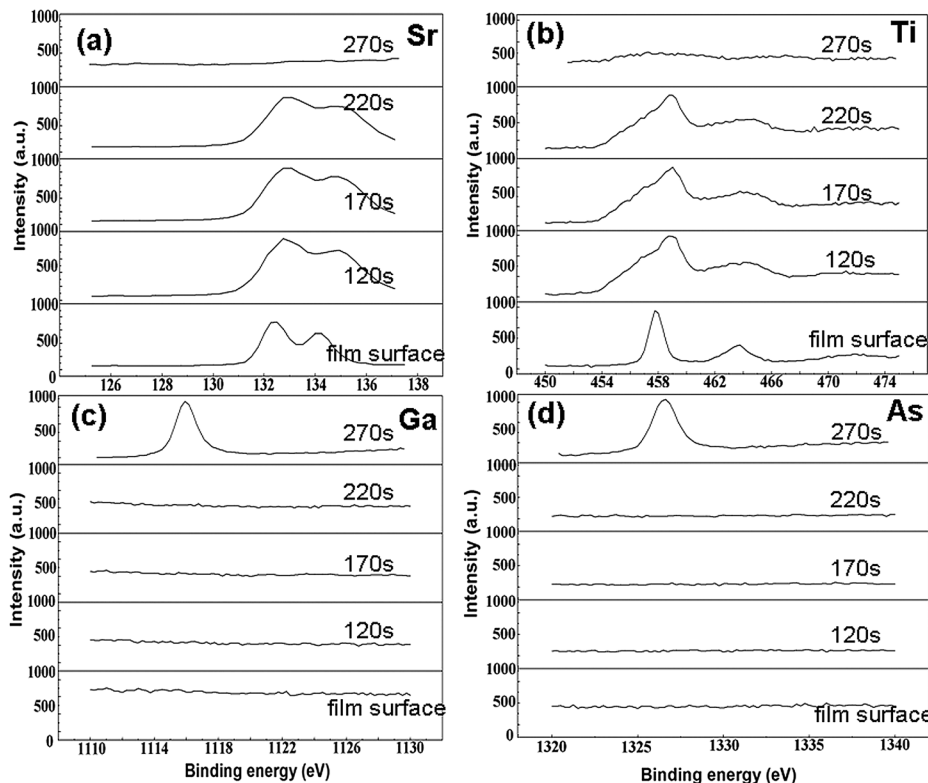
FIG. 4. XPS depth profile of core level spectra for STO/GaAs as function of sputtering time. Sr (a), Ti (b), Ga (c), and As (d).

According to the Ti *2p* spectra (Fig. 4(b)), the Ti $2p_{1/2}$ and Ti $2p_{3/2}$ lines indicative of Ti in 4^+ oxidation state become weak and finally disappear when the probing is completed from STO film surface to GaAs substrate. No other peaks and Ti line shift were observed. It indicates that it was fully oxidized in the film and no obvious Ti metallic compound was detected at the interface. Meanwhile, the typical lines of Ga $2p_{3/2}$ and As $2p_{3/2}$ are observed when the probing depth reaches GaAs substrate, as shown in Figs. 4(c) and 4(d). Furthermore, both typical peaks of Ga $2p_{3/2}$ and As $2p_{3/2}$ CL spectra are in agreement with earlier reported standard values of bulk GaAs.[24] Based on the observation, we could conclude that the heterostructure shows a sharp interface without interfacial compound in our highly epitaxial samples, which is consistent with the cross-sectional TEM image and our previous results of *in situ* reflective high energy electron diffraction (RHEED) patterns during the process of STO growth.[17,18] This fact could be attributed to the oxide target we used in laser deposition, while in MBE the metal was usually used as target. Wu *et al.* ever used density functional theory to evaluate the stable structure of Ti adsorbed on GaAs surfaces and found that the formation energies of Ti decreased with decreasing Ti coverage.[25] Furthermore, Sr atoms were adsorbed on the surface, whereas Ti atoms were adsorbed below the surface. In our case, the Sr and Ti atoms are relatively stable with oxidation states. It implies that the STO layer has indeed acted as a barrier against the oxidation of GaAs and vaporization of As from GaAs.

In summary, interfacial structure and phase of epitaxial STO thin film directly grown on GaAs have been investigated. According to the measured results by XPS and UPS, a type II band alignment diagram with a valence band offset of 2.6 eV and conduction band offset of 0.7 eV is obtained. The accurate determination of the band alignment of STO/GaAs in this work should be important for STO/GaAs based applications, such as high-*k* and ferroelectric microwave tunable devices. The XPS depth profile measurement is evident that the interface is free of interfacial compound in our epitaxial STO/GaAs heterostructure fabricated by laser deposition.

[1]M. Hong, J. Kwo, A. R. Kortan, J. P. Mannaerts, and A. M. Sergent, Science **283**, 1897 (1999).
[2]R. Chau, IEEE Trans. Nanotechnol. **4**, 153 (2005).
[3]M. Passlack, J. Abrokwah, R. Droopad, Z. Yu, C. Overgaard, S. Yi, M. Hale, J. Sexton, and A. Kummel, IEEE Electron Device Lett. **23**, 508 (2002).
[4]S. Oktyabrsky and P. D. Ye, *Fundamentals of III-V Semiconductor MOSFETs* (Springer, New York, 2010).
[5]W. C. Wang, K. Xiong, R. M. Wallace, and K. J. Cho, J. Phys. Chem. C **114**, 22610 (2010).
[6]K. Shubhakar, K. L. Pey, S. S. Kushvaha, S. J. O'Shea, N. Raghavan, M. Bosman, K. Kouda, K. Kakushima, and H. Iwai, Appl. Phys. Lett. **98**, 072902 (2011).
[7]S. Y. Yang, Q. Zhan, P. L. Yang, M. P. Cruz, Y. H. Chu, R. Ramesh, Y. R. Wu, J. Singh, W. Tian, and D. G. Schlom, Appl. Phys. Lett. **91**, 022909 (2007).
[8]L. W. Martin, Y.-H. Chu, Q. Zhan, R. Ramesh, S.-J. Han, S. X. Wang, M. Warusawithana, and D. G. Schlom, Appl. Phys. Lett. **91**, 172513 (2007).
[9]M. Hong, M. Passlack, J. P. Mannaerts, J. Kwo, S. N. G. Chu, N. Moriya, S. Y. Hou, and V. J. Fratello, J. Vac. Sci. Technol. B **14**, 2297 (1996).
[10]T. E. Murphy, D. Chen, and J. D. Phillips, Appl. Phys. Lett. **85**, 3208 (2004).
[11]D. Chen, T. E. Murphy, S. Chakrabarti, and J. D. Phillips, Appl. Phys. Lett. **85**, 5206 (2004).
[12]J. C. Le Breton, S. Le Gall, G. Jézéquel, B. Lépine, P. Schieffer, and P. Turban, Appl. Phys. Lett. **91**, 172112 (2007).
[13]Y. Liang, J. Kulik, T. C. Eschrich, R. Droopad, Z. Yu, and P. Maniar, Appl. Phys. Lett. **85**, 1217 (2004).
[14]R. Contreras-Guerrero, J. P. Veazey, J. Levy, and R. Droopad, Appl. Phys. Lett. **102**, 012907 (2013).
[15]Y. Liang, J. Curless, and D. McCready, Appl. Phys. Lett. **86**, 082905 (2005).
[16]J. H. Hao, J. Gao, Z. Wang, and D. P. Yu, Appl. Phys. Lett. **87**, 131908 (2005).
[17]W. Huang, Z. P. Wu, and J. H. Hao, Appl. Phys. Lett. **94**, 032905 (2009).
[18]Z. P. Wu, W. Huang, K. H. Wong, and J. H. Hao, J. Appl. Phys. **104**, 054103 (2008).
[19]L. S.-J. Peng, X. X. Xi, B. H. Moeckly, and S. P. Alpay, Appl. Phys. Lett. **83**, 4592 (2003).
[20]J. S. Wu, C. L. Jia, K. Urban, J. H. Hao, and X. X. Xi, J. Mater. Res. **16**, 3443 (2001).
[21]E. A. Kraut, R. W. Grant, J. R. Waldrop, and P. Kowalczyk, Phys. Rev. B **28**, 1965 (1983).
[22]K. Andreas, Thin Solid Films **520**, 3721 (2012).
[23]C. D. Wagner, W. M. Riggs, L. E. Davis, and G. E. Muilenberg, *A Reference Book of Standard Data for Use in X-Ray Photoelectron Spectroscopy* (Perkin-Elmer Corporation and Physical Electronics Divison, USA, 1979).
[24]S. McDonnell, H. Dong, J. M. Hawkins, B. Brennan, M. Milojevic, B. Brennan, M. Milojevic, F. S. Aguirre-Tostado, D. M. Zhernokletov, C. L. Hinkle, J. Kim, and R. M. Wallace, Appl. Phys. Lett. **100**, 141606 (2012).
[25]J. Wang, X. S. Wu, and D. Bai, Europhys. Lett. **86**, 46008 (2009).